

Original Research

# **Human NMO-IgG Induced Different Pathological and Immunological Changes in the CNS and Peripheral Tissues of Mice**

Weiwei Xiang<sup>1,†</sup>, Shuwei Bai<sup>1,†</sup>, Kan Wang<sup>1,†</sup>, Jing Peng<sup>1</sup>, Ze Wang<sup>1</sup>, Lu Han<sup>1</sup>, Chong Xie<sup>1,\*</sup>, Yangtai Guan<sup>1,\*</sup>

Submitted: 10 November 2023 Revised: 6 February 2024 Accepted: 18 February 2024 Published: 20 June 2024

#### Abstract

Objectives: The majority of neuromyelitis optica spectrum disorders (NMOSD) patients are seropositive for aquaporin-4 (AQP4)-specific antibodies [also named neuromyelitis optica immunoglobulin G antibodies (NMO-IgG)]. Although NMO-IgG can induce pathological changes in the central nervous system (CNS), the immunological changes in the CNS and peripheral tissue remain largely unknown. We investigated whether NMO-IgG binds to tissue expressing AQP4 and induces immunological changes in the peripheral tissue and CNS. Methods: C57BL/6 female mice were assigned into an NMOSD or control group. Pathological and immunological changes in peripheral tissue and CNS were measured by immunostaining and flow cytometry, respectively. Motor impairment was measured by open-field test. Results: We found that NMO-IgG did bind to astrocyte- and AQP4-expressing peripheral tissue, but induced glial fibrillary acidic protein and AQP4 loss only in the CNS. NMO-IgG induced the activation of microglia and modulated microglia polarization toward the classical (M1) phenotype, but did not affect innate or adaptive immune cells in the peripheral immune system, such as macrophages, neutrophils, Th17/Th1, or IL-10-producing B cells. In addition, NMOSD mice showed significantly less total distance traveled and higher immobility time in the open field. Conclusions: We found that injection of human NMO-IgG led to astrocytopathic lesions with microglial activation in the CNS. However, there were no significant pathological or immunological changes in the peripheral tissues.

Keywords: neuromyelitis optica spectrum disorders; aquaporin-4; microglia; pathological changes

# 1. Introduction

Neuromyelitis optica spectrum disorders (NMOSD) are inflammatory demyelinating disorders of the central nervous system (CNS) [1]. Although the incidence of NMOSD is relatively low, severe NMOSD attacks can lead to disability and mortality. Aquaporin-4 (AQP4) is highly expressed in astrocytes and peripheral tissue such as kidney collecting duct and skeletal muscle [2]. Most (70%) NMOSD patients are seropositive for AQP4-specific antibodies, which are also referred to as neuromyelitis optica immunoglobulin G antibodies (NMO-IgG) [3,4].

Current evidence supports the idea that NMO-IgG is pathogenic in NMOSD. For example, the levels of serum NMO-IgG are correlated with the severity of the disease in NMOSD patients, and plasma exchange that depletes NMO-IgG is clinically beneficial [5]. In the past decades, efforts have been made to develop animal models of NMOSD that mimic clinical and pathological features of NMOSD to varying degrees. Most of the reported NMOSD models involve systemic or direct injection of NMO-IgG into experimental animals, which induces neuroinflammation with astrocytopathic lesions and demyelination [6]. Recently, Hillebrand *et al.* [7] reported that systemic injection of NMO-IgG alone could breach the blood-

brain barrier (BBB) and induce pathological changes in the CNS. Taken together, the studies have provided compelling evidence for the pathogenicity of NMO-IgG.

Previous studies concerning the NMOSD model mainly focused on pathological effects in the CNS; the immunological changes in CNS and peripheral tissue induced by NMO-IgG were seldom studied. In the present study, we investigated whether systemically administered NMO-IgG would bind to tissue that expressed AQP4 and induce pathological changes. In addition, the immunological changes induced by NMO-IgG in peripheral tissue and the CNS were examined; we also tested for motor impairment in the treated subjects.

#### 2. Methods

# 2.1 NMO-IgG Purification

Plasma was obtained from healthy controls and NMOSD patients. AQP4-IgG was assessed by a cell-based indirect immunofluorescence assay. The plasma was obtained from acute NMOSD patients before the administration of any corticosteroids or other immunosuppressive therapy. NMO-IgG and control-IgG were purified using Melon Gel IgG Purification Kit (Thermo Fisher

<sup>&</sup>lt;sup>1</sup>Department of Neurology, Renji Hospital, Shanghai Jiao Tong University School of Medicine, 200127 Shanghai, China

<sup>\*</sup>Correspondence: xiechong6724@renji.com (Chong Xie); yangtaiguan@sina.com (Yangtai Guan)

<sup>&</sup>lt;sup>†</sup>These authors contributed equally. Academic Editor: Gernot Riedel

Scientific, Waltham, MA, USA), and further concentrated using Amicon Ultra-15 centrifugal filters (Merck Millipore, KGaA, Darmstadt, Germany). The protein concentration was determined by bicinchoninic acid assay (BCA) (Thermo Fisher Scientific), and the final concentration of IgG was adjusted to 20 mg/mL.

#### 2.2 Preparation of NMOSD Mice

C57BL/6 female mice (18–20 g, 6–8 weeks old, Shanghai Model Organisms Center, Shanghai, China) were used. The NMOSD mouse model was constructed as previously reported [8,9]. Mice were injected (s.c.) with an emulsion containing 4 mg/mL complete Freund's adjuvant (BD Difco, Franklin Lakes, NJ, USA) at 4 sites. Then, they were injected (i.p.) with 200 ng pertussis toxin (List Biological Laboratories, Campbell, CA, USA) on days 4 and 7 after immunization. Mice started to receive injections (i.p.) of NMO-IgG on day 0 for 8 consecutive days (5 mg NMO-IgG/day). The control group received injections of adjuvant, pertussis toxin, and the same amount of control-IgG.

#### 2.3 Detection of Motor Impairments

Motor impairment was graded by experimental allergic encephalomyelitis (EAE) score as previously described: stiff tail, 0.5; tail paralysis, 1; limp tail and waddling gait, 1.5; paralysis of one limb, 2; paralysis of one limb and weakness of another limb, 2.5; bilateral hind limb paralysis, 3; hind limb paralysis with forelimb weakness, 4; death, 5 [10]. Subtle locomotor abnormalities were assessed in the open field test (OFT). The OFT apparatus consisted of a plastic cage (420  $\times$  420  $\times$  420 mm) and a digital camera (Shanghai Soft maze Information Technology Co., Ltd., Shanghai, China). One hour before testing, mice were taken to the room for acclimation. The mouse was placed at the center of open field, and movement was recorded by the camera for 5 mins in order to examine distance traveled and duration of immobility. Before proceeding to the next trial, the open field was cleaned with 75 % ethanol.

### 2.4 Fluorescent Immunostaining

Mice were euthanized and perfused with phosphate buffer saline (PBS) and 4% paraformaldehyde. The spinal cords, optic nerves and brains were harvested. The tissue was cryosectioned and incubated with primary antibodies overnight at 4 °C: mouse anti-glial fibrillary acidic protein (Cell Signaling Technology, Danvers, MA, USA), rabbit anti-AQP4 (Sigma-Aldrich, St. Louis, MO, USA), rabbit anti-Iba-1 (Wako, Osaka, Japan). Sections were then washed with PBS and incubated with appropriate secondary antibody (Thermo Fisher Scientific) for 1 h at room temperature. Sections were stained with 4',6-diamidino-2-phenylindole (DAPI, Biolegend, Inc., San Diego, CA, USA) and visualized with a Leica microscope (Leica, Wetzlar, Germany). AQP4 and mouse anti-glial fibrillary acidic protein (GFAP) immunonegative areas were quantified us-

ing ImageJ software (1.8.0, National Institutes of Health, Bethesda, MD, USA).

#### 2.5 Flow Cytometry Analysis

Mice were anesthetized with tribromoethanol (M2940, Aibei biotechnology, Nanjing, Jiangsu, China) and perfused with cold PBS. The spinal cord and spleen were isolated and stored in hanks' balanced salt solution (HBSS) on ice until processing. The spinal cord was cut with sharp scissors and digested in a water bath at 37 °C for 30 min. The tissue was then homogenized with a plunger in fluorescence-activating cell sorter (FACS) buffer and centrifuged at 600 ×g for 5 min. The cell pellet was resuspended in 40% Percoll and centrifuged at 650 ×g for 30 min. The cells were washed twice and prepared for FACS using anti-CD11b, anti-CD45.2, anti-iNOS, anti-CD206 (Biolegend, Inc., San Diego, CA, USA) antibodies. The spleen was homogenized and centrifuged at 350 ×g for 5 min. The supernatant was aspired and the pellet was re-suspended in the red-cell lysis buffer for 5 min on ice. FACS buffer was used to stop the lysis reaction. The cells were acquired and prepared for FACS. For intracellular interferon (IFN)- $\gamma$ , interleukin (IL)-17, and IL-10 staining, cells were stimulated with phorbol myristate acetate (PMA, Sigma-Aldrich, St. Louis, MO, USA), ionomycin (Sigma-Aldrich, St. Louis, MO, USA), and monensin (Thermo Fisher Scientific, Waltham, MA, USA) for 4 h. Flow cytometry was performed using a FACS celesta (BD Bioscience, San Jose, CA, USA), and data were analyzed by FlowJo software (Tree Star, Ashland, OR, USA).

#### 2.6 Statistics

Variables were checked for normality before analysis. Differences between 2 groups were analyzed by a 2-tailed unpaired Student's t test or Mann-Whitney U test. Data were presented as mean  $\pm$  standard deviation (SD). Calculation was performed using GraphPad Prism software (GraphPad, La Jolla, CA, USA, v. 8.0). A p < 0.05 was regarded as statistically significant.

## 3. Results

#### 3.1 NMO-IgG Induced Subtle Motor Impairment

To determine the effects of NMO-IgG on motor function, the EAE scoring system was used. All NMOSD mice showed stiff tails on day 8, with only one NMOSD mouse showing a waddling gait on day 5, but the motor dysfunction resolved on day 6. Subtle locomotor abnormalities in NMOSD mice were measured in the OFT. As shown in Fig. 1, NMOSD mice had significantly less total distance traveled (p < 0.001) and longer immobility duration than did the control group (p < 0.001).



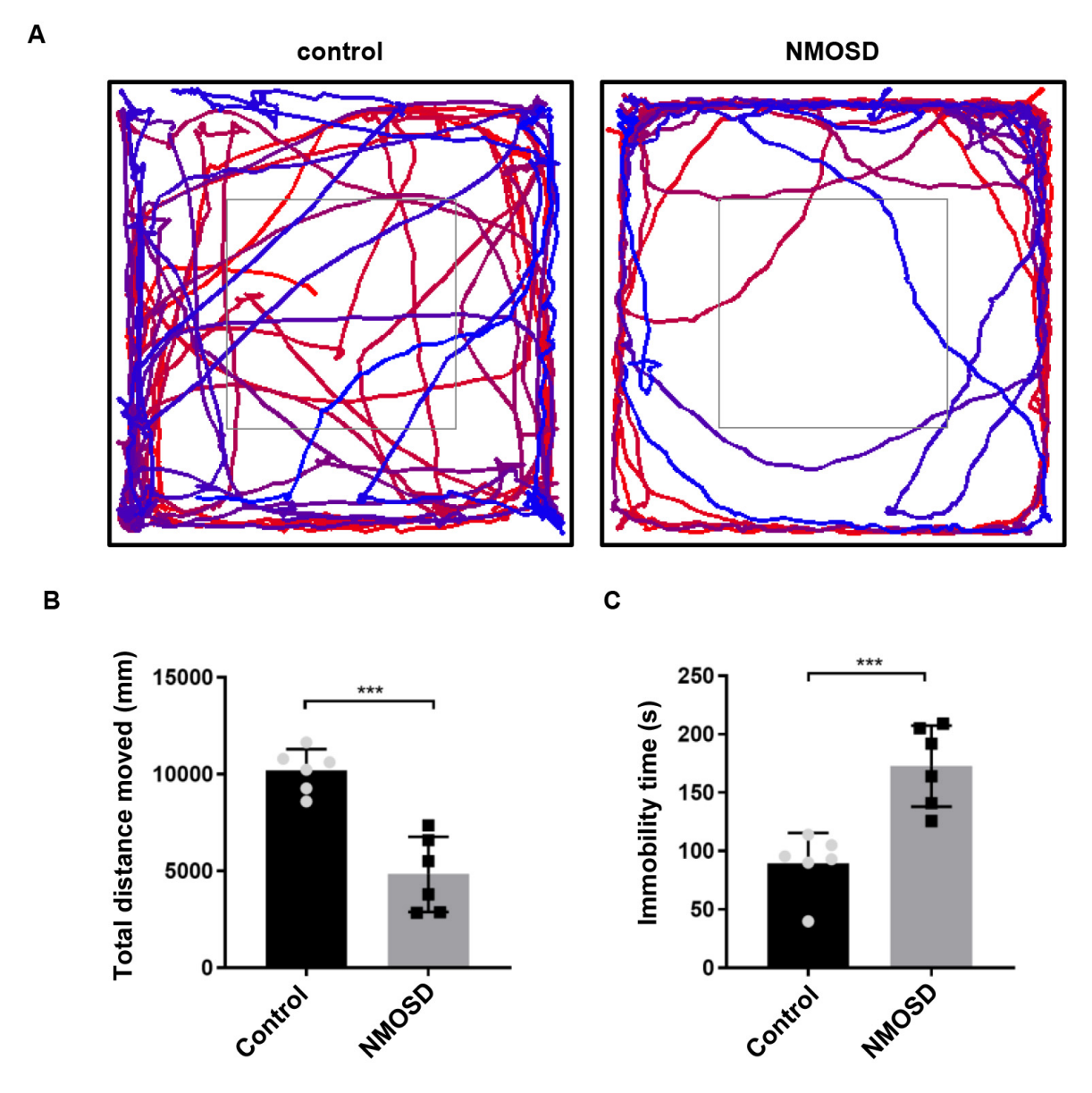


Fig. 1. Subtle motor impairments of NMOSD mice detected by open field test. (A) Graphical representation of the walking paths of control and NMOSD mice. (B,C) Total distance traveled and immobility time of mice on OFT. \*\*\*p < 0.001. Data are presented as mean  $\pm$  standard deviation (SD). n = 6/gp. NMOSD, neuromyelitis optica spectrum disorders; OFT, open field test.

# 3.2 NMO-IgG Infiltrated the Spinal Cord Parenchyma and Caused AQP4 and GFAP Loss

Human IgG staining revealed that NMO-IgG infiltrated the spinal cord parenchyma; the deposition of IgG was mainly restricted to the perivascular space, pericentral canal, and subpial space (Fig. 2A). Furthermore, IgG/GFAP double staining showed that the NMO-IgG bound to astrocytes in the spinal cord parenchyma (Fig. 2B). These results confirmed that systemically administrated NMO-IgG infiltrated the spinal cord parenchyma via the breached BBB.

To examine the effect of NMO-IgG on the expression of AQP4 and GFAP, immunofluorescence analyses were performed. Results showed that GFAP (p < 0.0001) and AQP4 (p < 0.0001) were significantly lower in the spinal

cord white matter of NMOSD mice than in control mice (Fig. 3A,B). Furthermore, we evaluated NMO-IgG-induced astrocytopathy in the optic nerve. As shown in Fig. 3C,D, GFAP (p < 0.01) and AQP4 (p < 0.01) were also significantly lower in the optic nerve of NMOSD mice than in control mice.

# 3.3 NMO-Ig-Induced Microglia Activation

Immunostaining revealed markedly higher numbers of Iba-1<sup>+</sup> cells in the spinal cord of NMOSD mice than in control mice (p < 0.01) (Fig. 4A,B), whereas there was no significant difference in the number of Iba-1<sup>+</sup> cells in the brain (Fig. 4C,D). Although inducible nitric oxide synthase (iNOS<sup>+</sup>) microglia numbers were also higher in the experimental group (p < 0.01), no significant difference



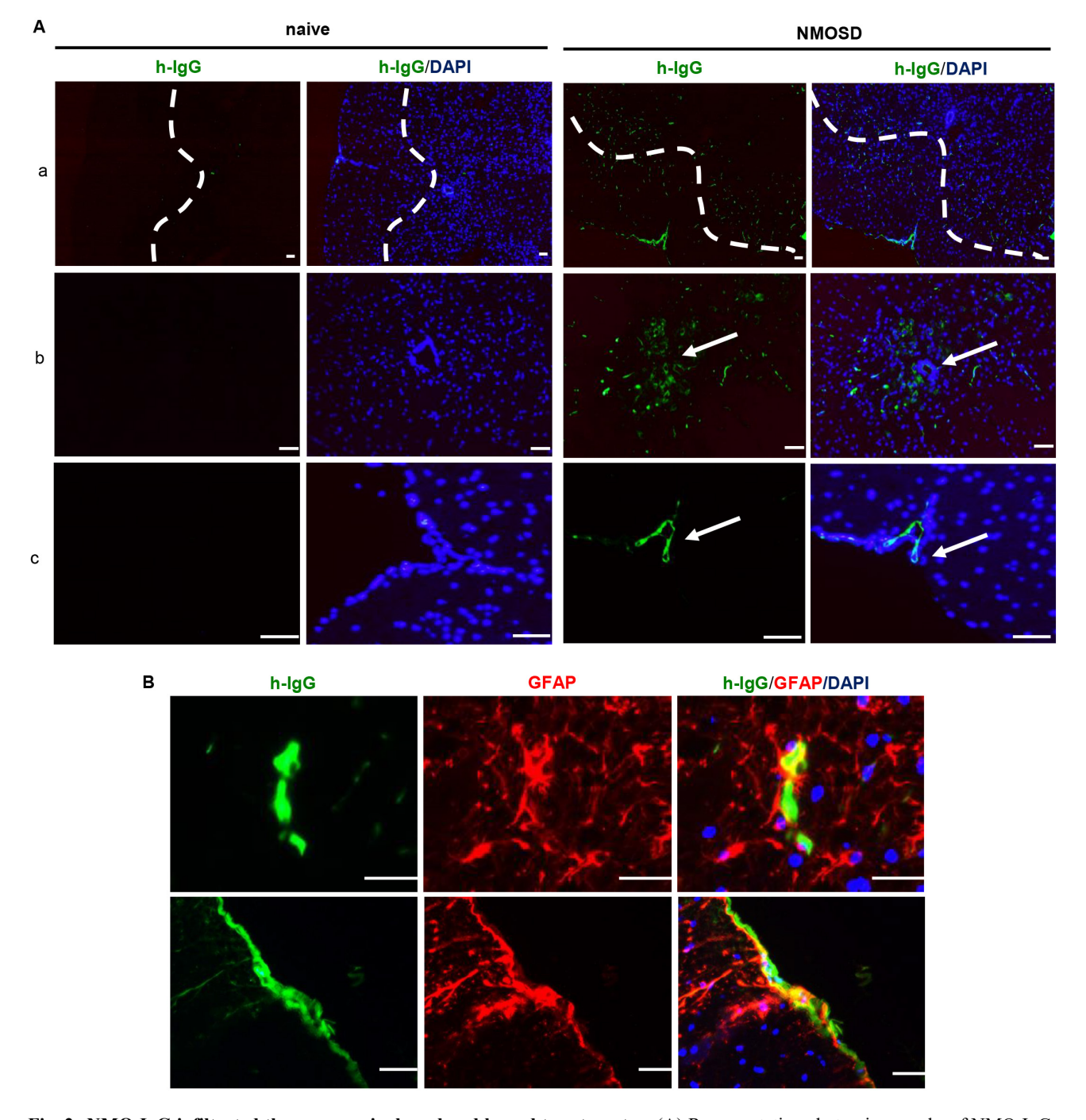


Fig. 2. NMO-IgG infiltrated the mouse spinal cord and bound to astrocytes. (A) Representative photomicrographs of NMO-IgG infiltrated spinal cord parenchyma. (a) Deposition of NMO-IgG in the spinal cord parenchyma around perivascular space; (b) deposition of NMO-IgG in the pericentral canal; (c) deposition of NMO-IgG in the subpial space. (B) NMO-IgG bound to astrocytes in NMOSD mice. Scale bar =  $50 \mu m$ . NMO-IgG, neuromyelitis optica immunoglobulin G antibodies; DAPI, 4',6-diamidino-2-phenylindole; GFAP, glial fibrillary acidic protein.

was found in CD206<sup>+</sup> microglia between the two groups (p = 0.6943) (Fig. 4E–H). We also conducted hematoxylin and eosin (H&E) staining on spinal cord, brain and optic nerve slices and found on differences in inflammatory cells between NMOSD and control groups (**Supplementary Fig. 1**).

3.4 NMO-IgG Bound to Peripheral Tissue that Expressed AOP4

Peripheral distribution of NMO-IgG was evaluated after 8 days of i.p. injections. We examined whether NMO-IgG bound to the peripheral organs that expressed AQP4 and induced changes. As shown in Fig. 5, AQP4 was expressed on the basolateral membrane of the kidney collect-



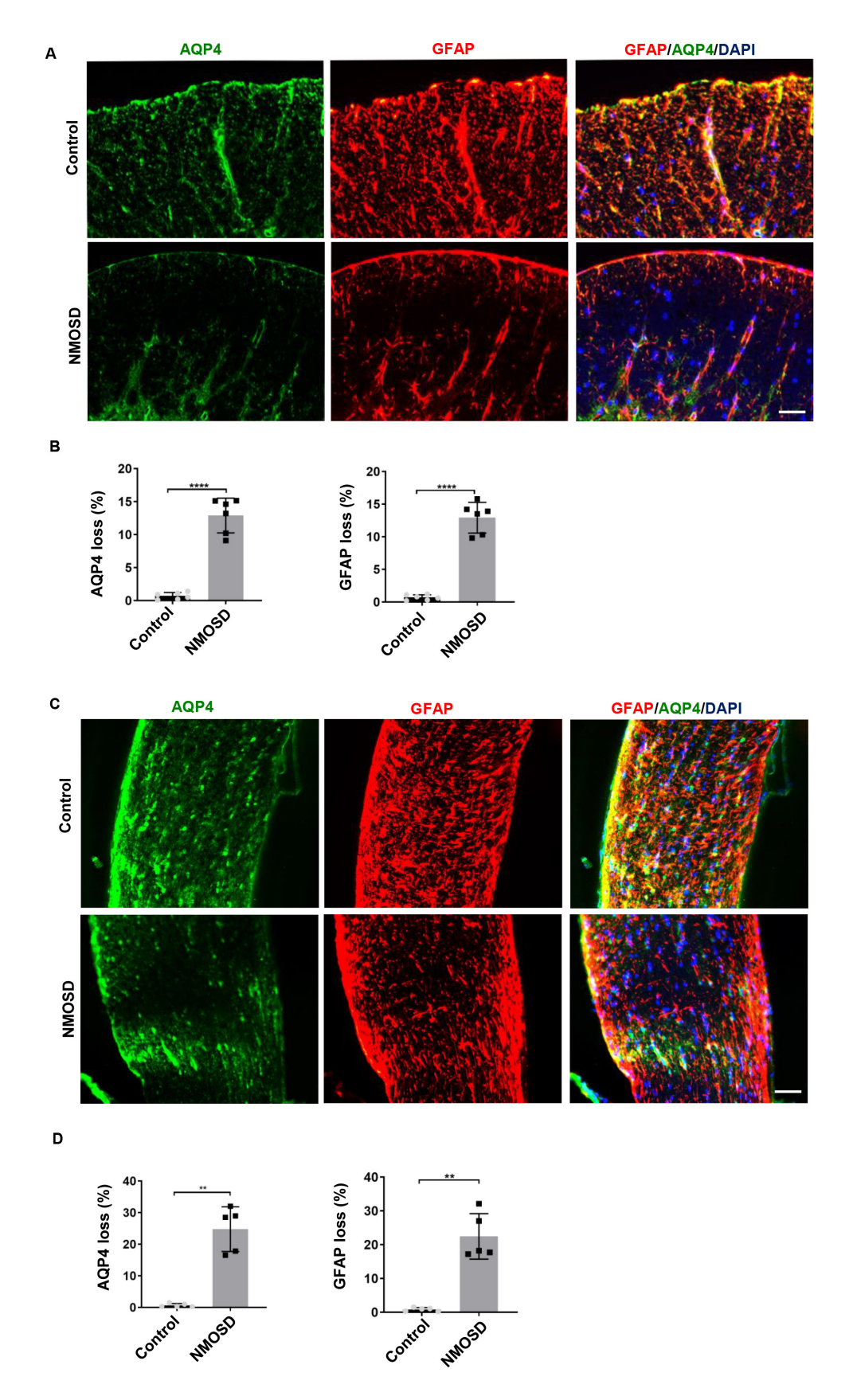


Fig. 3. NMO-IgG caused AQP4 and GFAP loss. (A,C) Loss of AQP4 and GFAP in the spinal cord and optic nerve of NMOSD mice and control mice; (B,D) The statistical results of the AQP4 and GFAP loss between the two groups, n = 5-6/gp. \*\*p < 0.01; \*\*\*\*p < 0.0001. Data are presented as mean  $\pm$  SD. Scale bar = 50  $\mu$ m. AQP4, aquaporin-4; GFAP, glial fibrillary acidic protein.

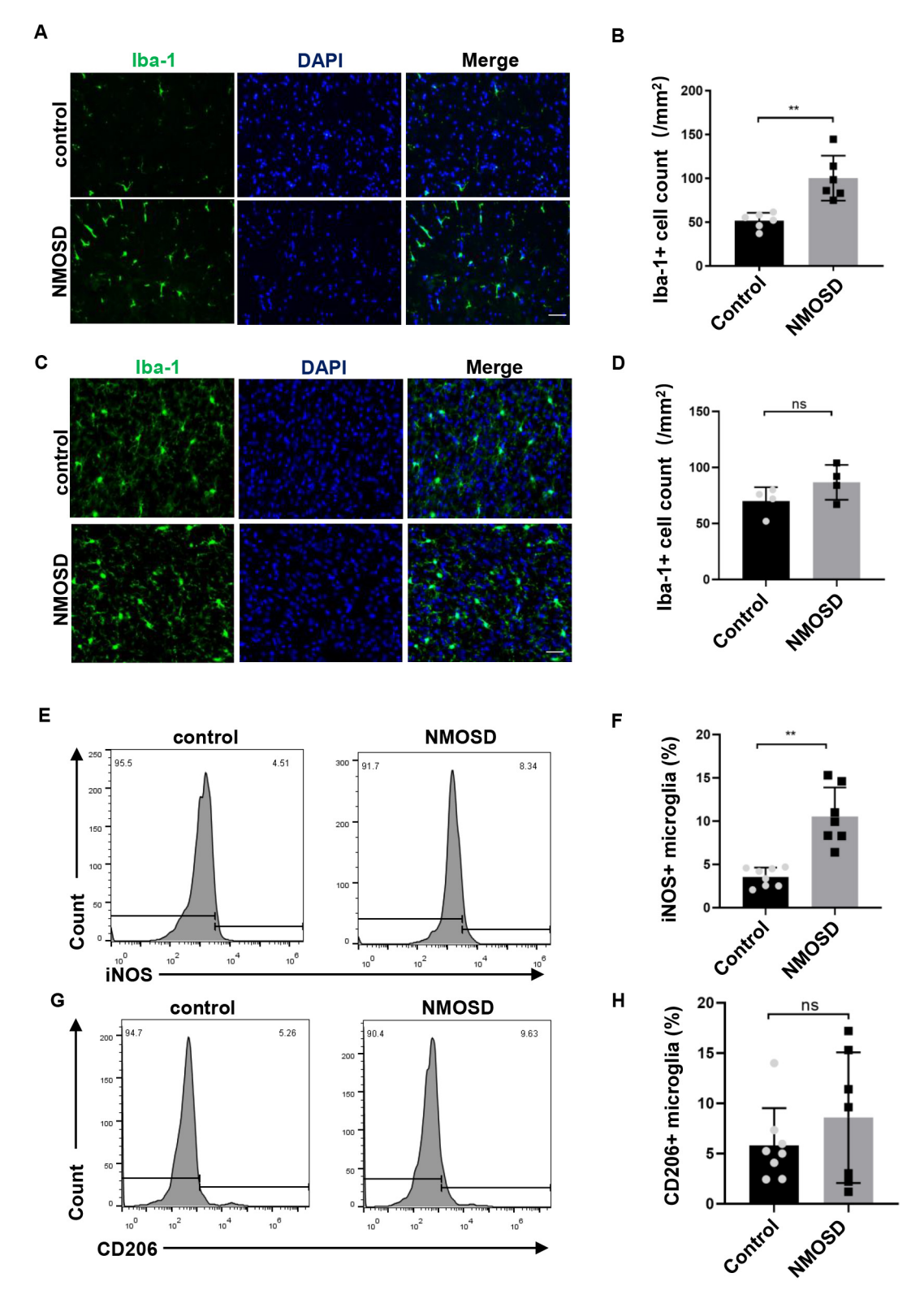


Fig. 4. NMO-IgG modulated microglia polarization toward M1. (A,C) Immunofluorescence staining for Iba-1 in the spinal cord and brain of NMOSD and control mice, Scale bar =  $50 \mu m$ ; (B,D) The statistical results of the number of Iba-1<sup>+</sup> cells between the two groups, n = 4-6/gp; (E,F) Histogram curves of the expression of the inducible nitric oxide synthase (iNOS) in the microglia, and the statistical results, n = 7-8/gp; (G,H) Histogram curves of the expression of the CD206 in the microglia, and statistical results, n = 7-8/gp. ns = no significant difference; Data are presented as the mean  $\pm$  SD; \*\*p < 0.01.

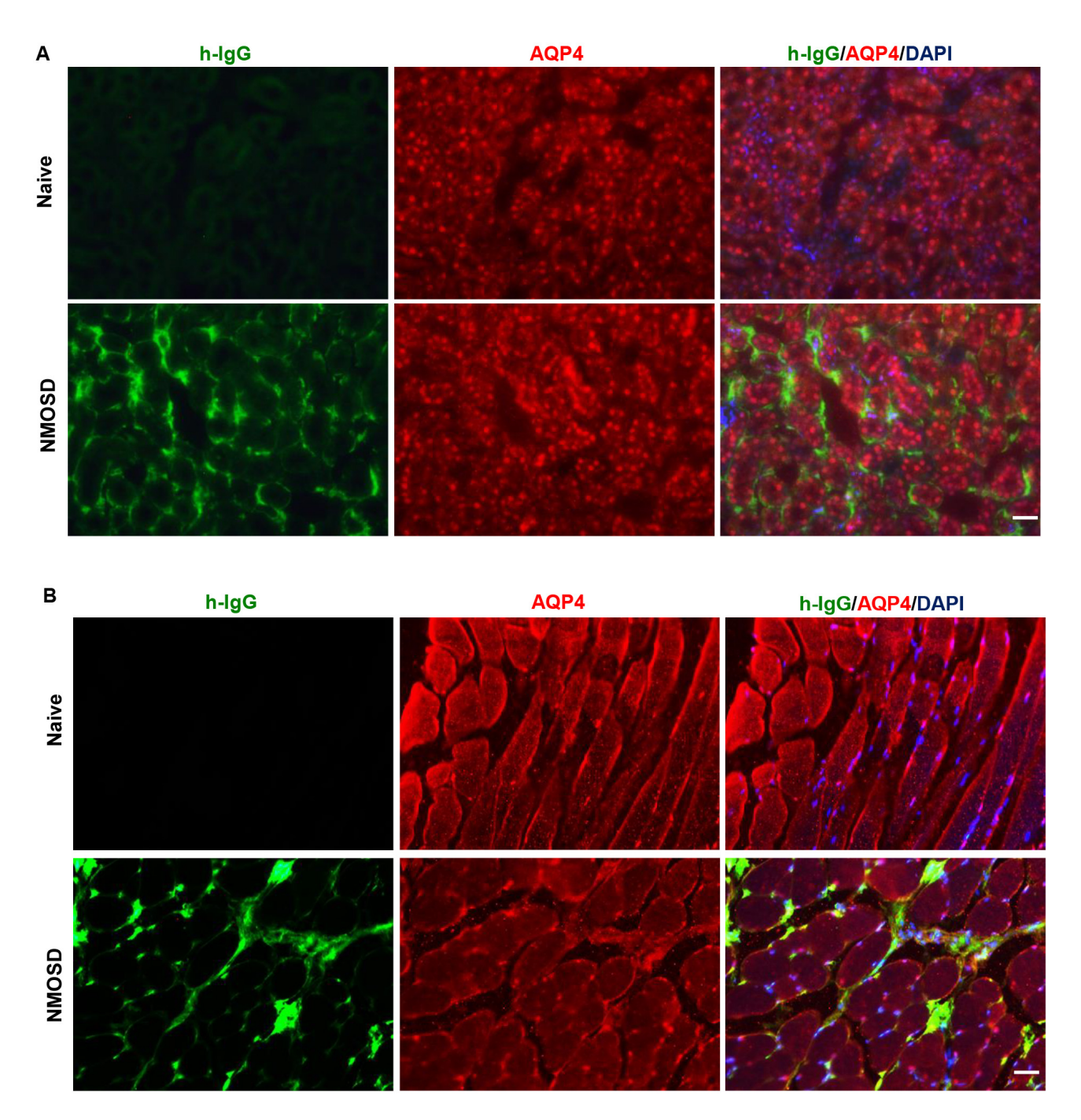


Fig. 5. NMO-IgG localization to peripheral tissues that expressed AQP4. (A) IgG/AQP4 double immunostaining revealed NMO-IgG bound to the basal side of kidney collecting duct cells. (B) NMO-IgG localization to plasmalemma of skeletal muscle in NMOSD mice. Scale bar =  $50 \mu m$ .

ing duct and on the plasmalemma of skeletal muscle of naïve mice. IgG/AQP4 double immunostaining revealed that NMO-IgG bound to the basal side of kidney-collecting-duct cells and to the plasmalemma of skeletal muscle in NMOSD mice. However, there was no difference in the AQP4 immunoreactivities between the NMOSD and naïve mice, which indicated that tissue damage was not induced by NMO-IgG.

3.5 NMO-IgG did not Affect the Percentage of Peripheral Immune Cells in the Spleen

To determine the effect of NMO-IgG on peripheral immune cells, we performed flow cytometry on the spleen. As shown in Fig. 6, no significant differences were found in the percentage of macrophages/neutrophils of NMOSD and control mice (p=0.3446 and p=0.2128, respectively). Splenocytes were also stimulated *ex vivo* for 4 h, and stained with antibodies for the flow cytometric analy-



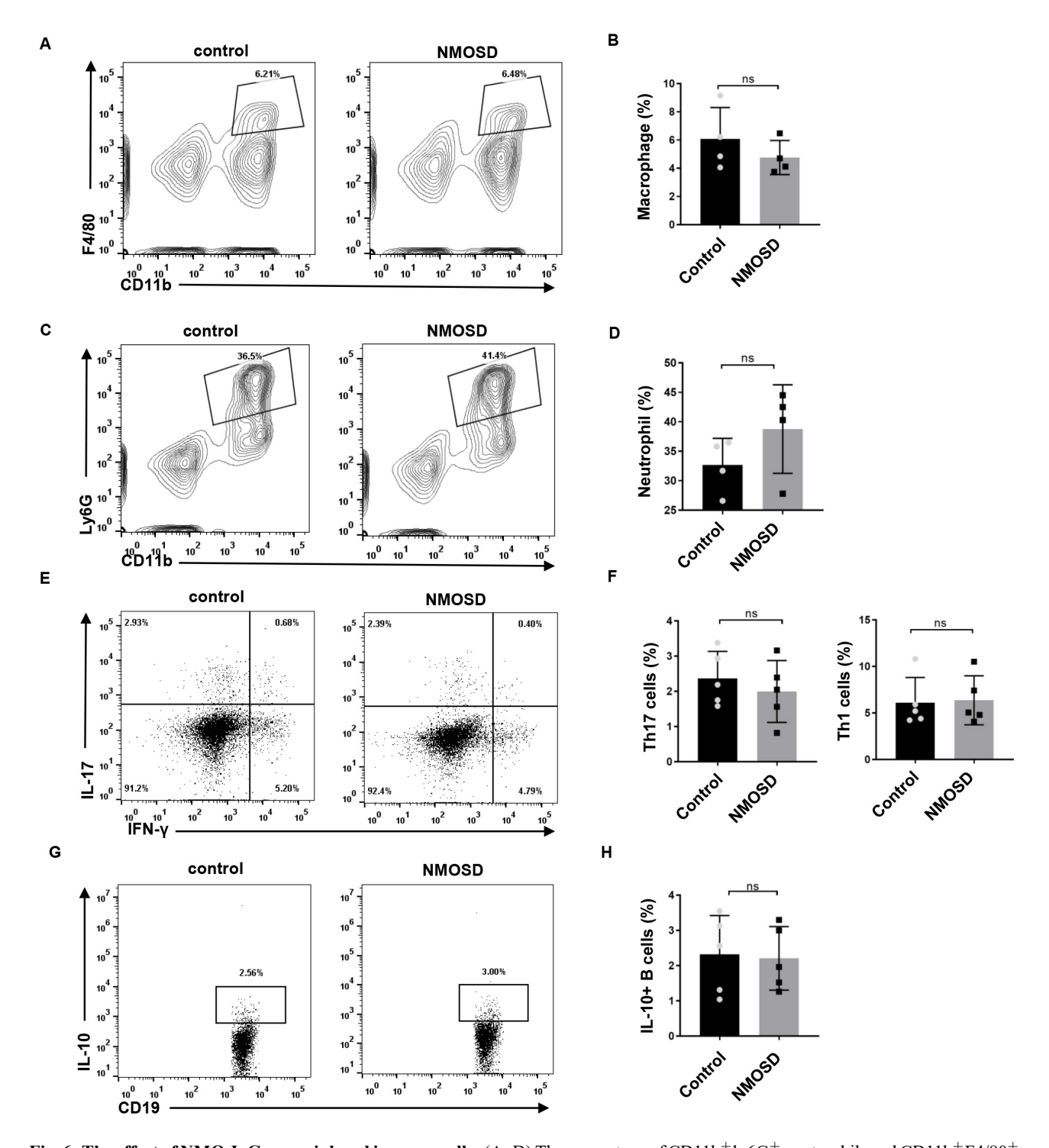


Fig. 6. The effect of NMO-IgG on peripheral immune cells. (A–D) The percentage of CD11b<sup>+</sup>ly6G<sup>+</sup> neutrophils and CD11b<sup>+</sup>F4/80<sup>+</sup> macrophages and the statistical results. (E,F) Flow cytometric analysis of IFN- $\gamma^+$  and IL-17A<sup>+</sup> cells in CD4<sup>+</sup> T cells. (G,H) The percentage of IL-10<sup>+</sup> cells in CD19<sup>+</sup> B cells and the statistical results. ns = no significant difference; Data are presented as the mean  $\pm$  SD; n = 4–5/gp. IL, interleukin; IFN- $\gamma$ , interferon- $\gamma$ .

sis of Th17/Th1 and IL-10-producing B cells. We found no significant differences in the percentage of IL-17 (p = 0.4990) and IFN- $\gamma$  secreting CD4<sup>+</sup> T cells (p = 0.8824). Additionally, there was no significant difference in the percentage of IL-10-producing B cells between the two groups (p = 0.8674).

# 4. Discussion

Current animal models of NMOSD can be divided into two types: systemic-injection models and direct-injection models [6]. In the present study, by using a systemic injection NMOSD model, we revealed that injected NMO-IgG infiltrated the CNS parenchyma and induced GFAP and



AQP4 loss. Although NMO-IgG did bind to the peripheral tissue that expressed AQP4, such as kidney and skeletal muscle, it had no effect on AQP4 immunoreactivity in those peripheral tissues. In addition, NMO-IgG triggered activation of microglia and modulated microglia polarization toward M1 in the CNS, but did not affect the percentage of peripheral immune cells.

Our results showed that all NMOSD mice had tiff tails. Consistently, OFT revealed impaired locomotive activity in NMOSD mice; they showed significantly less total distance traveled and greater immobility time than did the control mice. As NMO-IgG did not induce any detectable pathological changes in peripheral AQP4-expressing tissues, the motor abnormalities can be ascribed to the observed astrocytopathic lesions in the spinal cord. Together, the manifestations of NMOSD in the experimental mice recapitulated the mild myelitis observed in some NMOSD patients.

NMO-IgG is rarely detected exclusively in cerebrospinal fluid of NMOSD patients, and NMO-IgG in the CNS was generally thought to originate from circulating peripheral NMO-IgG via a disrupted BBB [11]. Previous studies demonstrated that 24 h after systemic injection, NMO-IgG could be found in the area postrema of mice [12,13]. In the present study, we found a deposition of NMO-IgG in the spinal cord parenchyma around the perivascular space, pericentral canal, and subpial space. Hillebrand *et al.* [7] also reported diffused infiltration of NMO-IgG in the CNS. They speculated that NMO-IgG may use three different avenues of entry into the CNS, including meningeal vessels, parenchymal vessels, and circumventricular organs.

Because AQP4 is also highly expressed outside the CNS, we studied NMO-IgG localization in peripheral tissues [2]. Tissue-distribution studies showed that NMO-IgG had bound to the basal side of kidney-collecting-duct cells and to the plasmalemma of skeletal muscle in the NMOSD mice, without affecting the AQP4 immunoreactivities. Consistent with our study, Hillebrand *et al.* [7] systemically administered highly pathogenic, monoclonal NMO-IgG to rats and found autoantibodies bound to AQP4-expressing peripheral tissue. The difference though, was that they found decreased AQP4 expression in those tissues [7]. This difference may be ascribed to the highly pathogenic, monoclonal NMO-IgG they used, whereas human NMO-IgG is typically polyclonal with different affinities.

Microglia are usually the first responders to pathogen invasion or CNS damage. Emerging evidence has revealed the important role of microglia in NMOSD pathogenesis [14]. There is prominent activation of microglia in the CNS of NMOSD patients, as indicated by the amoeboid morphology and the expression of lysosome marker CD68 [15]. In the present study, there was significantly greater microglial activation in NMOSD mice than in control mice. The observed activation of microglia in NMOSD mice was

likely to have been mediated by astrocyte-driven microglial activation. NMO-IgG was reported to have bound to the AQP4 of astrocytes and induced the activation of astrocytes, which in turn drove the activation of microglia; microglial activation was abrogated when NMO-IgG was injected into AQP4 knockout mice [16]. Under different micro-environmental disturbances, the activated microglia could polarize into either the classical (M1) or alternative (M2) phenotype, and exert a pro-inflammatory or anti-inflammatory role, respectively [17]. In the present study, we found that NMO-IgG induced microglia polarization toward M1, which may have participated in the pathological role of NMO-IgG in NMOSD mice.

Autoantibodies can trigger a diverse set of effector responses in peripheral myeloid cells, such as neutrophils and macrophages. In the present study, we examined whether splenic macrophages and neutrophils could be activated in response to human NMO-IgG. We observed no significant difference in the percentage of macrophages or neutrophils between the two groups. Consistently, Pellerin et al. [18] reported that anti-myelin oligodendrocyte glycoprotein antibodies triggered the activation of microglia but not the activation of peripheral macrophages. The frequency of Th17 cells and IL-10-producing B cells in NMOSD patients was reported to be significantly different from that of healthy controls [19-22]. However, our results showed no statistical differences in these cells between NMOSD and control mice, which may be explained by the fact the NMO-IgG were injected, not self-generated by mice.

#### 5. Conclusions

In the present study, we found that human NMO-IgG injection led to astrocytopathic lesions with microglial activation in the CNS. However, there were no significant pathological and immunological changes in the peripheral tissues.

#### Availability of Data and Materials

The datasets generated during the current study are available from the corresponding author on reasonable request.

# **Author Contributions**

WWX: Conceptualization, Methodology, Investigation, Writing - original draft. KW: Conceptualization, Methodology, Investigation. SWB: Conceptualization, Methodology, Investigation. ZW: Visualization, Investigation. LH: Visualization, Investigation. JP: Visualization, Investigation, Investigation, Supervision, Writing - review & editing. YTG: Conceptualization, Supervision. All authors contributed to editorial changes in the manuscript. All authors read and approved the final manuscript. All authors have participated sufficiently in the work and agreed to be accountable for all aspects of the work.



# **Ethics Approval and Consent to Participate**

This study was reviewed and approved by Ethics Committee of the Renji Hospital Affiliated to Shanghai Jiao Tong University School of Medicine (KY2021-137-B). The provided the written informed consents of patients/participants were obtained. All experimental procedures were approved by the Shanghai Model Organisms Center's Ethical Committee.

#### Acknowledgment

Not applicable.

# **Funding**

This work was supported by the National Natural Science Foundation of China (81801195), Innovative research team of high-level local universities in Shanghai (SHSMU-ZDCX20211901) and Shanghai "Rising Stars of Medical Talents" Youth Development Program.

#### **Conflict of Interest**

The authors declare no conflict of interest.

# **Supplementary Material**

Supplementary material associated with this article can be found, in the online version, at https://doi.org/10.31083/j.jin2306119.

#### References

- [1] Pittock SJ, Lucchinetti CF. Neuromyelitis optica and the evolving spectrum of autoimmune aquaporin-4 channelopathies: a decade later. Annals of the New York Academy of Sciences. 2016; 1366: 20–39.
- [2] Ratelade J, Bennett JL, Verkman AS. Intravenous neuromyelitis optica autoantibody in mice targets aquaporin-4 in peripheral organs and area postrema. PLoS ONE. 2011; 6: e27412.
- [3] Lennon VA, Wingerchuk DM, Kryzer TJ, Pittock SJ, Lucchinetti CF, Fujihara K, *et al.* A serum autoantibody marker of neuromyelitis optica: distinction from multiple sclerosis. Lancet (London, England). 2004; 364: 2106–2112.
- [4] Lennon VA, Kryzer TJ, Pittock SJ, Verkman AS, Hinson SR. IgG marker of optic-spinal multiple sclerosis binds to the aquaporin-4 water channel. The Journal of Experimental Medicine. 2005; 202: 473–477.
- [5] Bonnan M, Valentino R, Olindo S, Mehdaoui H, Smadja D, Cabre P. Plasma exchange in severe spinal attacks associated with neuromyelitis optica spectrum disorder. Multiple Sclerosis (Houndmills, Basingstoke, England). 2009; 15: 487–492.
- [6] Duan T, Verkman AS. Experimental animal models of aquaporin-4-IgG-seropositive neuromyelitis optica spectrum disorders: progress and shortcomings. Brain Pathology (Zurich, Switzerland). 2020; 30: 13–25.
- [7] Hillebrand S, Schanda K, Nigritinou M, Tsymala I, Böhm D, Peschl P, et al. Circulating AQP4-specific auto-antibodies alone

- can induce neuromyelitis optica spectrum disorder in the rat. Acta Neuropathologica. 2019; 137: 467–485.
- [8] Chan KH, Zhang R, Kwan JSC, Guo VY, Ho PWL, Ho JWM, et al. Aquaporin-4 autoantibodies cause asymptomatic aquaporin-4 loss and activate astrocytes in mouse. Journal of Neuroimmunology. 2012; 245: 32–38.
- [9] Yick LW, Tang CH, Ma OKF, Kwan JSC, Chan KH. Memantine ameliorates motor impairments and pathologies in a mouse model of neuromyelitis optica spectrum disorders. Journal of Neuroinflammation. 2020; 17: 236.
- [10] Xie C, Li X, Zhou X, Li Z, Zhang Y, Zhao L, *et al.* TGFβ1 transduction enhances immunomodulatory capacity of neural stem cells in experimental autoimmune encephalomyelitis. Brain, Behavior, and Immunity. 2018; 69: 283–295.
- [11] Akaishi T, Takahashi T, Misu T, Kaneko K, Takai Y, Nishiyama S, *et al.* Difference in the Source of Anti-AQP4-IgG and Anti-MOG-IgG Antibodies in CSF in Patients With Neuromyelitis Optica Spectrum Disorder. Neurology. 2021; 97: e1–e12.
- [12] Bradl M, Misu T, Takahashi T, Watanabe M, Mader S, Reindl M, et al. Neuromyelitis optica: pathogenicity of patient immunoglobulin in vivo. Annals of Neurology. 2009; 66: 630–643.
- [13] Asavapanumas N, Verkman AS. Neuromyelitis optica pathology in rats following intraperitoneal injection of NMO-IgG and intracerebral needle injury. Acta Neuropathologica Communications. 2014; 2: 48.
- [14] Chen T, Bosco DB, Ying Y, Tian DS, Wu LJ. The Emerging Role of Microglia in Neuromyelitis Optica. Frontiers in Immunology. 2021; 12: 616301.
- [15] Lucchinetti CF, Guo Y, Popescu BFG, Fujihara K, Itoyama Y, Misu T. The pathology of an autoimmune astrocytopathy: lessons learned from neuromyelitis optica. Brain Pathology (Zurich, Switzerland). 2014; 24: 83–97.
- [16] Chen T, Lennon VA, Liu YU, Bosco DB, Li Y, Yi MH, et al. Astrocyte-microglia interaction drives evolving neuromyelitis optica lesion. The Journal of Clinical Investigation. 2020; 130: 4025–4038.
- [17] Tang Y, Le W. Differential Roles of M1 and M2 Microglia in Neurodegenerative Diseases. Molecular Neurobiology. 2016; 53: 1181–1194.
- [18] Pellerin K, Rubino SJ, Burns JC, Smith BA, McCarl CA, Zhu J, *et al.* MOG autoantibodies trigger a tightly-controlled FcR and BTK-driven microglia proliferative response. Brain: a Journal of Neurology. 2021; 144: 2361–2374.
- [19] Varrin-Doyer M, Spencer CM, Schulze-Topphoff U, Nelson PA, Stroud RM, Cree BAC, et al. Aquaporin 4-specific T cells in neuromyelitis optica exhibit a Th17 bias and recognize Clostridium ABC transporter. Annals of Neurology. 2012; 72: 53–64.
- [20] Yokote H, Yagi Y, Watanabe Y, Amino T, Kamata T, Mizusawa H. Serum amyloid A level is increased in neuromyelitis optica and atypical multiple sclerosis with smaller T2 lesion volume in brain MRI. Journal of Neuroimmunology. 2013; 259: 92–95.
- [21] Sun Y, Huang Y, Chen WW, Jia J, Wei T. The IL-10-producing regulatory B cells (B10 cells) and regulatory T cell subsets in neuromyelitis optica spectrum disorder. Neurological Sciences: Official Journal of the Italian Neurological Society and of the Italian Society of Clinical Neurophysiology. 2018; 39: 1307– 1308
- [22] Quan C, ZhangBao J, Lu J, Zhao C, Cai T, Wang B, et al. The immune balance between memory and regulatory B cells in NMO and the changes of the balance after methylprednisolone or rituximab therapy. Journal of Neuroimmunology. 2015; 282: 45–53.

